Dicle University
Journal of Engineering

https://dergipark.org.tr/tr/pub/dumf
duje.dicle.edu.tr

Research Article

Model Predictive Trajectory Tracking Control of 2 DoFs SCARA Robot under External Force Acting to the Tip along the Trajectory

Sertaç Emre KARA[1], Osman YİĞİD[2], Murat ŞEN[3], Mesut HÜSEYİNOĞLU[4*]

[1] Fırat University, Mechanical Engineering Department, sekara@firat.edu.tr, Orcid No: 0000-0001-7463-5867
[2] Fırat University, Mechanical Engineering Department, yigidosman@gmail.com, Orcid No: 0000-0002-1798-1250
[3] Fırat University, Mechanical Engineering Department, msen@firat.edu.tr, Orcid No: 0000-0002-3063-5635
[4] Dicle University, Mechanical Engineering Department, mesuth@dicle.edu.tr, Orcid No: 0000-0002-6130-6658

ARTICLE INFO

Article history:

Received 28 April 2023
Received in revised form 08 June 2023
Accepted 14 June 2023
Available online 19 June 2023

Keywords:

2 DoFs SCARA robot, trajectory control, model predictive control

Doi: 10.24012/dumf.1289356

* Corresponding author

ABSTRACT

The robot arms often follow a certain trajectory depending on the type of end effector with functions of spray-painting, arc welding, bonding or machining etc. Therefore, trajectory-tracking control is a very important issue in robot arm applications. Also, the robot must be able to follow the determined trajectory stably under the influence of external forces or machining forces it encounters in its operations. In this study, a Model Predictive Control (MPC) for trajectory tracking control of a 2 Degrees of Freedom (DoFs) Selective Compliant Assembly Robot Arm (SCARA) under an external force acting to the tip of the robot along the trajectory was performed. The effectiveness of the MPC method used has been demonstrated by simulation applications. According to simulation studies, successful results were obtained.

Introduction

Robot arms are widely used in industrial application areas to do certain operations like welding, painting, proper positioning systems, etc. In these operations, the end effectors of the robot arms are required to move from one point to another or to follow certain trajectories as closely as possible. Trajectory tracking control is used to achieve desired trajectories. The motion tracking control of robots is one of the difficulties because of uncertainties such as load variations, friction, external disturbances, unknown nonlinearities, and a time-varying dynamics system. Therefore, trajectory-tracking control has become the most fundamental research area in the control of robot arms. Many algorithms and methods in the literature have been proposed and performed to keep accurate position control and stability in robot arms.

Computed torque control is an efficient motion control approach for robotic manipulators [1]. Wijesoma and Richards [2] suggested a method for robust accurate trajectory tracking of manipulators based on the computed torque method and variable-structure systems (VSS) theory. Researchers also use computed torque control for parallel manipulators [3], and master-slave robot manipulator systems [4]. Artificial intelligence methods compared to analytical methods are widely used for motion control of manipulators. Saad et al. [5] investigated the trajectory-tracking problem to control the nonlinear dynamic model of the SCARA robot with 2 Degrees of Freedom (2 DoFs) using a DSP-based controller based on neural networks. The controllers rely on learning from input-output measurements rather than dynamics based on parametric models. An adaptive neuro controller for robot manipulators based on the radial basis function network is suggested by Lee and Choi [6]. Sun and Wang [7] proposed an approach based on an adaptive fuzzy control strategy for robot manipulators. The control system is constructed by combining three methods that are an independent joint control strategy, generating initial rules, and online parameter optimization through learning. An adaptive decentralized control strategy was described by Hsu and Fu [8] for the tracking control of robot manipulators driven by current-fed induction motors. With this strategy, all signals of closed-loop systems are limited to eliminate all parametric uncertainties. In another study [9], a control method called the fuzzy-based generalized predictive control is applied to a nonlinear system to overcome the limitations of the PID and the linear generalized predictive control in operating points that differed from the controller design specification. The studies of control strategy for robot motion control based on fuzzy logic and artificial neural networks are also given in [10-14]. Sliding Mode Control (SMC), Proportional-Integral-Derivative (PID), and adaptive PID control methods have been used effectively in robot motion control. Huseyinoglu and Abut [15] implemented the SMC and PID control methods to control the 2 DoFs robot arm. The dynamic statements of the robot arm are derived by using the Lagrange-Euler method. A brand-new kind of fuzzy-sliding mode controller is addressed in [16]. To provide certain predictable performances, a sliding mode controller for robust tracking is initially created on the presumption that imposed system uncertainties fulfill matching conditions. Mustafa [17] presented a study using the three PID techniques for the control of the 2-Revelutejoint robot. A PID control law depends on neural networks and fuzzy PID controllers have been used in trajectory tracking control of two DoF robot arms [18]. Evolutionary algorithms (EAs) have emerged as an alternative design technique for robot motion control applications [19] and [20]. Real-time sliding mode and PID control of triglide robot and RCM mechanism are presented in [21] and [22]. Abut and Soyguder [23] used the adaptive computed torque control method for real-time control of bilateral teleoperation system. Then, they applied the optimal adaptive computed torque control method to haptic teleoperation robotic systems in order to eliminate dynamic uncertainty, which is one of the main problems in haptic systems [24].

Many researchers have used the Model Predictive Control (MPC) method [25-27], which provides a more robust control for robot trajectory. The basic concept of this control approach is to predict the future behavior of a system up to a determined finite prediction horizon time by minimizing the finite horizon cost function defined under the future states with some determined constraints. Although the history of MPC dates back to Zadeh and Whalen [28] and Propoi [29], its popularity has gradually increased with its use in the chemical process industry [30-31]. This control method generally relies on a system attempting to predict the future behavior of the system for each step in a defined horizon. While doing this, it is ensured that the horizon objective function created is minimized under certain constraints [32]. Houzhang et al. [33], studied controlling a vehicle semi-active suspension system by using an explicit model predictive control approach in which the control law computation requirement is low. Some researchers used MPC for controlling mobile robots and autonomous ground vehicles under some determined vehicles [34-35]. Guechi et al. [36], resented a comparative control study of a planar two DoFs robot arm by using MPC and LQ control methods. The nonlinear dynamic equations of the robot were linearized by using the feedback linearization method and the MPC control parameters were optimized analytically minimizing a cost function.

In this study, trajectory tracking control of 2 DoFs Selective Compliant Assembly Robot Arm (SCARA) under external force acting on the tip along the trajectory is performed by using the MPC method.

Kinematic and Dynamic Equations of 2 DoFs SCARA Robot

In this section, the kinematic and dynamic equations are given for 2 DoFs SCARA robot. The parameters and the coordinates of the robot are illustrated in Figure 1 below.

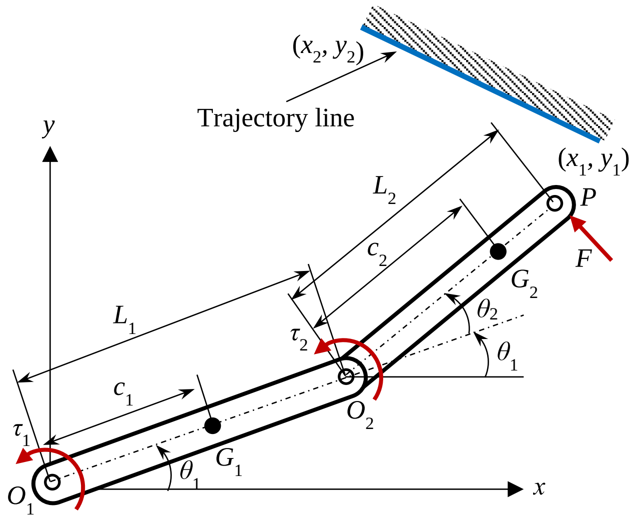

Figure 1. 2 DoFs SCARA robot arm.

As seen in Figure 1, an external force (F) is applied to the endpoint of the robot through the trajectory line. This force is assumed to be perpendicular to link 2. The generalized coordinates for link 1 and link 2 are θ1 and θ2, the torques are τ1 and τ2 respectively. The lengths of the links are L1 and L2, and the positions of the center of gravity (G1, G2) of the links c1 and c2. The position of the endpoint of the robot in the x-y coordinate system can be calculated by using Equation 1 with the angular displacements and the dimensions of the links.

$$\begin{aligned} x &= L_1\cos(\theta_1) + L_2\cos(\theta_1+\theta_2) \\ y &= L_1\sin(\theta_1) + L_2\sin(\theta_1+\theta_2) \end{aligned} \tag{1}$$

For a prescribed endpoint position in the x-y plane (in the limits of the robot workspace), the required angular displacements can be calculated by using Equation 2. The kinetic and potential energy terms for a 2 DoFs robot can be written for the links with Equation (3)

$$\begin{aligned} \theta_2 &= \cos^{-1}\left(\frac{x^2+y^2-L_1^2-L_2^2}{2L_1L_2}\right) \\ \theta_1 &= \tan^{-1}\left(\frac{y(L_1+L_2\cos\theta_2)-xL_2\sin\theta_2}{x(L_1+L_2\cos\theta_2)+yL_2\sin\theta_2}\right) \end{aligned} \tag{2}$$

$$\begin{aligned} T_1 &= \frac{1}{2}(m_1c_1^2+I_1)\dot{\theta}_1^2 \\ U_1 &= m_1gc_1\sin\theta_1 \\ T_2 &= \frac{1}{2}m_2\begin{pmatrix} L_1^2\dot{\theta}_1^2 + c_2^2\left(\dot{\theta}_1+\dot{\theta}_2\right)^2 + \cdots \\ \cdots 2L_1\dot{\theta}_1c_2\left(\dot{\theta}_1+\dot{\theta}_2\right)\cos\theta_2 + \cdots \\ \cdots\frac{1}{2}I_2\left(\dot{\theta}_1+\dot{\theta}_2\right)^2 \end{pmatrix} \\ U_2 &= m_2g(L_1\sin\theta_1 + c_2\sin(\theta_1+\theta_2)) \end{aligned} \tag{3}$$

$$\tau_1 = \begin{pmatrix} (\alpha + 2\beta\cos\theta_2)\ddot{\theta}_1 + (\delta + \beta\cos\theta_2)\ddot{\theta}_2 - \cdots \\ \cdots \beta\sin\theta_2\dot{\theta}_1\dot{\theta}_2 - \beta\sin\theta_2\left(\dot{\theta}_1 + \dot{\theta}_2\right)\dot{\theta}_2 \end{pmatrix} \quad (4)$$
$$\tau_2 = (\delta + \beta\cos\theta_2)\ddot{\theta}_1 + \delta\ddot{\theta}_2 + \beta\sin\theta_2\dot{\theta}_1^2$$

The equations of motion of the SCARA robot are obtained by using Lagrange Function as follows:

Where,

$$\begin{aligned} \alpha &= I_1 + I_2 + m_1c_1^2 + m_2(L_1^2 + c_2^2) \\ \beta &= m_2L_1c_2 \\ \delta &= I_2 + m_2c_2^2 \end{aligned} \quad (5)$$

The equations given in Equation 4 are non-linear and do not contain potential energy terms as the SCARA robot moves in the parallel plane to the ground. It can be rearranged in compact form as follow:

$$M\ddot{\theta} + C = \tau \quad (6)$$

Where,

$$\begin{aligned} M &= \begin{bmatrix} \alpha + 2\beta\cos\theta_2 & \delta + \beta\cos\theta_2 \\ \delta + \beta\cos\theta_2 & \delta \end{bmatrix} \\ \ddot{\theta} &= \{\ddot{\theta}_1 \quad \ddot{\theta}_2\}^T \\ C &= \begin{bmatrix} -2\beta\sin\theta_2\,\dot{\theta}_1\dot{\theta}_2 - \beta\sin\theta_2\,\dot{\theta}_2^2 \\ \beta\sin\theta_2\,\dot{\theta}_1^2 \end{bmatrix} \\ \tau &= \{\tau_1 \quad \tau_2\}^T \end{aligned} \quad (7)$$

Equation 6 is obtained for the system without an external force. For an external force that is applied to the robot tip as given in Figure 2, the effect of the force can be obtained using the virtual work approach. The virtual displacements of the tip concerning the joints can be written as in Equation (8) and Equation (9).

$$\begin{aligned} \delta R_{O_2P}^x &= -L_2\sin(\theta_1 + \theta_2)\delta(\theta_1 + \theta_2) \\ \delta R_{O_2P}^y &= L_2\cos(\theta_1 + \theta_2)\delta(\theta_1 + \theta_2) \end{aligned} \quad (8)$$

$$\begin{aligned} \delta R_{O_1P}^x &= -L_1\sin\theta_1\,\delta\theta_1 - L_2\sin(\theta_1 + \theta_2)\delta(\theta_1 + \theta_2) \\ \delta R_{O_1P}^y &= L_1\cos\theta_1\,\delta\theta_1 + L_2\cos(\theta_1 + \theta_2)\delta(\theta_1 + \theta_2) \end{aligned} \quad (9)$$

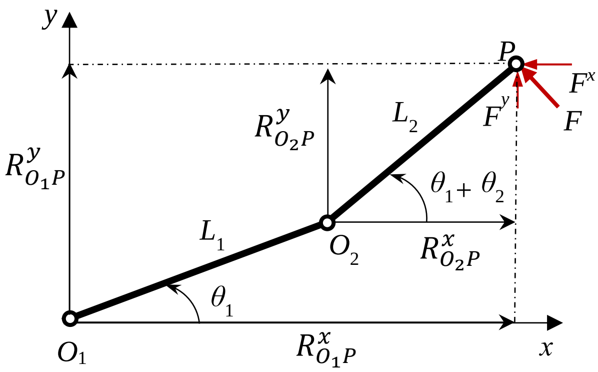

Figure 2. The position vectors of the tip according to the joints

The virtual works done by the applied force to the tip can be determined with Equation (10).

$$\begin{aligned} Q_1 &= F^x\delta R_{O_2P}^x + F^y\delta R_{O_2P}^y \\ Q_2 &= F^x\delta R_{O_1P}^x + F^y\delta R_{O_1P}^y \end{aligned} \quad (10)$$

The total virtual work can be obtained with Equation (11).

$$\begin{aligned} Q &= Q_1 + Q_2 \\ &= \begin{pmatrix} F^x(-L_1\sin\theta_1\,\delta\theta_1 - 2L_2\sin(\theta_1 + \theta_2)\delta(\theta_1 + \theta_2)) \\ \cdots F^y(L_1\cos\theta_1\,\delta\theta_1 + 2L_2\cos(\theta_1 + \theta_2)\delta(\theta_1 + \theta_2) \end{pmatrix} \end{aligned} \quad (11)$$

The calculated moments acting on Joint 1 and Joint 2 can be obtained with partial differential concerning θ_1 and θ_2.

$$T_{\theta_1} = \frac{\partial Q}{\partial \theta_1} = \begin{pmatrix} F^x(-L_1\sin\theta_1 - L_1\cos\theta_1\,\delta\theta_1 - 2L_2\sin(\theta_1 + \theta_2) - 2L_2\cos(\theta_1 + \theta_2)\,\delta(\theta_1 + \theta_2)) + \cdots \\ \cdots F^y(L_1\cos\theta_1 - L_1\sin\theta_1\,\delta\theta_1 + 2L_2\cos(\theta_1 + \theta_2) - 2L_2\sin(\theta_1 + \theta_2)\,\delta(\theta_1 + \theta_2)) \end{pmatrix} \quad (12)$$
$$T_{\theta_2} = \frac{\partial Q}{\partial \theta_2} = \begin{pmatrix} F^x(-2L_2\sin(\theta_1 + \theta_2) - 2L_2\cos(\theta_1 + \theta_2))\delta(\theta_1 + \theta_2) + \cdots \\ \cdots F^y(2L_2\cos(\theta_1 + \theta_2) - 2L_2\sin(\theta_1 + \theta_2)\,\delta(\theta_1 + \theta_2)) \end{pmatrix}$$

The dynamic model of the robot with tip force is rearranged as follows.

$$M\ddot{\theta} + C + T = \tau \quad , \quad T = \{T_{\theta_1} \quad T_{\theta_2}\}^T \quad (13)$$

MPC Controller Design

In this section, the design of the MPC controller, which is designed to follow the trajectory under the influence of an external force acting on the tip of the SCARA robot, whose general motion equations are given by Equation (14) is given. Model predictive control (MPC) as mentioned in previous sections is a robust control method that minimizes a cost function with some constraints for dynamical systems through a finite horizon time [32]. The concept of this control method depends on the prediction of the future response of the examined dynamic system for each instance up to horizon time by minimizing a cost function. An MPC control block diagram is illustrated in Figure 3 schematically, where r, u, y, and z represent the desired input, control signal, output, and disturbances respectively.

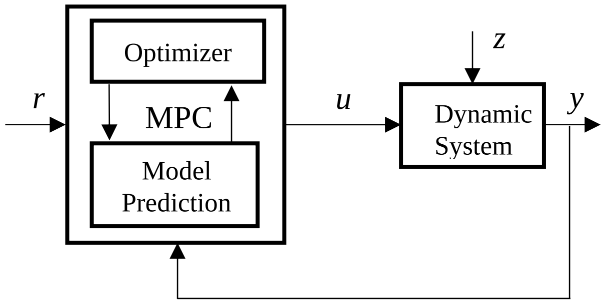

Figure 3. MPC controller system block diagram.

Equation (13) can be written as follows, together with the related variables.

$$M(\theta)\ddot{\theta} + C(\theta, \dot{\theta}) + T(\theta) = \tau \qquad (14)$$

The error functions can be written as follows where subscript (d) represents the desired condition.

$$\begin{aligned} e(t) &= \theta_d(t) - \theta(t) \\ \dot{e}(t) &= \dot{\theta}_d(t) - \dot{\theta}(t) \\ \ddot{e}(t) &= \ddot{\theta}_d(t) - \ddot{\theta}(t) \end{aligned} \qquad (15)$$

By rearranging Equation 14, the following expression can be obtained.

$$\ddot{\theta} = M(\theta)^{-1}\left(\tau - C(\theta, \dot{\theta}) - T(\theta)\right) \qquad (16)$$

Where u is the synthetic control vector as follows [36]:

$$u = \{u_1 \quad u_2\}^T \qquad (17)$$

The actual control torque can be written by using this synthetic control torque with Equation (18).

$$\tau = M(\theta)u + C(\theta, \dot{\theta}) + T(\theta) \qquad (18)$$

The linearized decoupled equations are given as follows:

$$\begin{aligned} \ddot{\theta}_1 &= u_1 \\ \ddot{\theta}_2 &= u_2 \end{aligned} \qquad (19)$$

In the case of the selection of the control law as proportional-derivative (PD) [36].

$$\begin{aligned} u_1 &= k_1(\theta_{1d} - \theta_1) + k_2(\dot{\theta}_{1d} - \dot{\theta}_1) \\ u_2 &= k_3(\theta_{2d} - \theta_2) + k_4(\dot{\theta}_{2d} - \dot{\theta}_2) \end{aligned} \qquad (20)$$

Where,

$$\begin{aligned} k_1 &= \omega_1^2 \; ; \; k_2 = 2\zeta_1\omega_1 \\ k_3 &= \omega_2^2 \; ; \; k_4 = 2\zeta_2\omega_2 \end{aligned} \qquad (21)$$

Using Equations (15-16) the following linearized expression can be written for input to the system.

$$u = \ddot{\theta}_d + M(\theta)^{-1}\left(C(\theta, \dot{\theta}) + T(\theta) - \tau\right) \qquad (22)$$

Then the computed torque can be expressed with Equation (23).

$$\tau = M(\theta)(\ddot{\theta}_d - u) + C(\theta, \dot{\theta}) + T(\theta) \qquad (23)$$

The input torque can be obtained using the control law as follows.

$$\tau = M(\theta)(\ddot{\theta}_d + K_d\dot{e} + K_p e) + C(\theta, \dot{\theta}) + T(\theta) \quad (24)$$

The prediction model can be written in the determined time interval with horizon t to t+h assuming $u(t)$=u is constant as follows:

$$\begin{aligned} \dot{\theta}_1(t + h_1) &= u_1 h_1 + \dot{\theta}_1(t) \\ \theta_1(t + h_1) &= \frac{1}{2}u_1 h_1^2 + \dot{\theta}_1(t)h_1 + \theta_1(t) \\ \dot{\theta}_2(t + h_2) &= u_2 h_2 + \dot{\theta}_2(t) \\ \theta_2(t + h_2) &= \frac{1}{2}u_2 h_2^2 + \dot{\theta}_2(t)h_2 + \theta_2(t) \end{aligned} \qquad (25)$$

With constant reference angles, the cost functions can be written with Equation (23).

$$\begin{aligned} J_1 &= e_1^2(t + h_1) + \rho_1\dot{e}_1^2(t + h_1) \\ J_2 &= e_2^2(t + h_2) + \rho_2\dot{e}_2^2(t + h_2) \end{aligned} \qquad (26)$$

Here, ρ_1 and ρ_2 are the weight factors. The required control gains can be calculated with Equation (27).

$$\begin{aligned} k_1 &= \frac{2}{h_1^2 + 4\rho_1} \; ; \; k_2 = \frac{2h_1^2 + 4\rho_1}{h_1^3 + 4\rho_1 h_1} \\ k_3 &= \frac{2}{h_2^2 + 4\rho_2} \; ; \; k_4 = \frac{2h_2^2 + 4\rho_2}{h_2^3 + 4\rho_2 h_2} \end{aligned} \qquad (27)$$

Using Equation (21) the following expressions can be obtained.

$$\frac{\theta_1(s)}{\theta_{1d}(s)} = \frac{k_1}{s^2 + k_2 s + k_1} ; \frac{\theta_2(s)}{\theta_{2d}(s)} = \frac{k_3}{s^2 + k_4 s + k_3} \quad (28)$$

Equation (29) can be written using Equation (21) and Equation (28) [36].

$$\begin{aligned} 2\zeta_1\omega_1 &= \frac{2h_1^2 + 4\rho_1}{h_1^3 + 4\rho_1 h_1} \; ; \; \omega_1^2 = \frac{2}{h_1^2 + 4\rho_1} \\ 2\zeta_2\omega_2 &= \frac{2h_2^2 + 4\rho_2}{h_2^3 + 4\rho_2 h_2} \; ; \; \omega_2^2 = \frac{2}{h_2^2 + 4\rho_2} \end{aligned} \qquad (29)$$

The weight factors can be calculated with Equation (30).

$$\rho_1 = \frac{2 - \omega_1^2 h_1^2}{4\omega_1^2} \; ; \; \rho_2 = \frac{2 - \omega_2^2 h_2^2}{4\omega_2^2} \qquad (30)$$

The roots of the equations obtained by substituting Equation (30) into Equation (29) can be calculated as follows [36].

$$\begin{aligned} \lambda_{1,2} &= 2\zeta_1 \pm \sqrt{4\zeta_1^2 - 2} \\ \lambda_{3,4} &= 2\zeta_2 \pm \sqrt{4\zeta_2^2 - 2} \end{aligned} \tag{31}$$

From Equation (31), for the positive weight factors Equation (32) can be written.

$$\begin{aligned} 2(4\zeta_1^2 - 2) - \zeta_1\sqrt{4\zeta_1^2 - 2} < 0 \\ 2(4\zeta_2^2 - 2) - \zeta_2\sqrt{4\zeta_2^2 - 2} < 0 \end{aligned} \tag{32}$$

By choosing ζ_1, ζ_2, ω_1 and ω_2 as design parameters, h_1, and h_2 can be determined.

Trajectory Control Simulations

In this section, some simulation studies are given to show the effectiveness of the MPC method for control applications of the SCARA robot. The physical and mechanical parameters of the robot used for simulation studies are given in Table 1.

For simulation studies, a trajectory line illustrated in Figure 1 was created between two points in the workplace of the robot as (x_1=0.438, y_1=0.315; x_2=0.168, y_2=0.491). The external force was assumed to be perpendicular to link 2 through the trajectory line. The linear position graphs with and without external force are obtained for both the actual and the desired conditions comparatively in Figure 4.

Table 1. The physical and mechanical parameters of the SCARA robot.

Parameters	Values
L_1: Length of link 1 (m)	0.390
L_2: Length of link 1 (m)	0.156
c_1: Center of gravity of link 1 (m)	0.195
c_2: Center of gravity of link 2 (m)	0.078
m_1: Mass of link 1 (kg)	3.3
m_1: Mass of link 2 (kg)	0.3
I_1: Mass moment of inertia for center of gravity link 1 (kgm^2)	0.12550
I_2: Mass moment of inertia for center of gravity link 2 (kgm^2)	0.00183
F: External force (N)	1
θ_1: Rotational displacement of link 1	(degree)
θ_2: Rotational displacement of link 2	(degree)
τ_1: Torque of link 1	(Nm)
τ_2: Torque of link 2	(Nm)

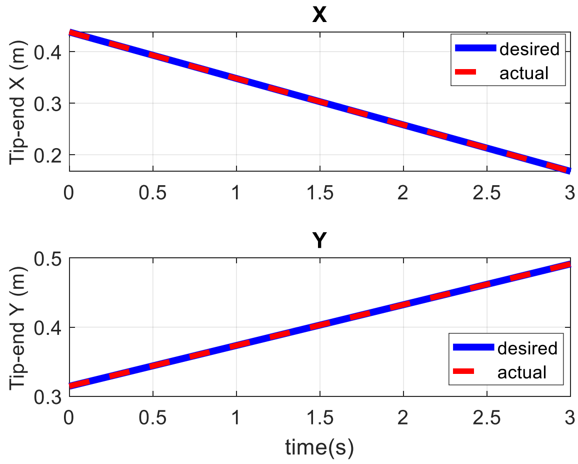

(a)

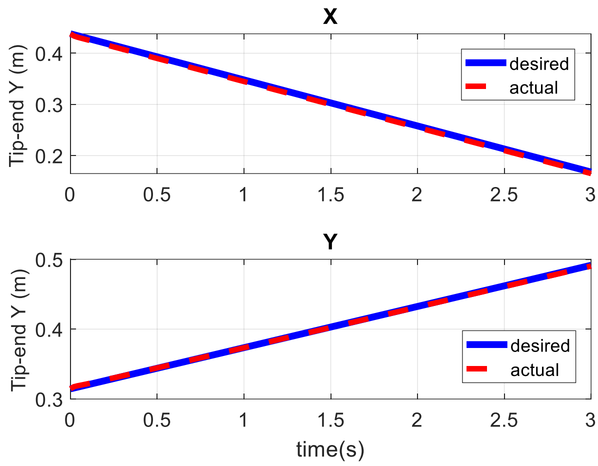

(b)

Figure 4. Comparison of the linear positions of the actual and desired conditions for each link (a) without external force, (b) with external force.

In addition, the angular positions for the desired and the obtained conditions are given in Figure 5. The required torques for the trajectory tracking through the determined trajectory line are given in Figure 6 for free and with external force conditions comparatively.

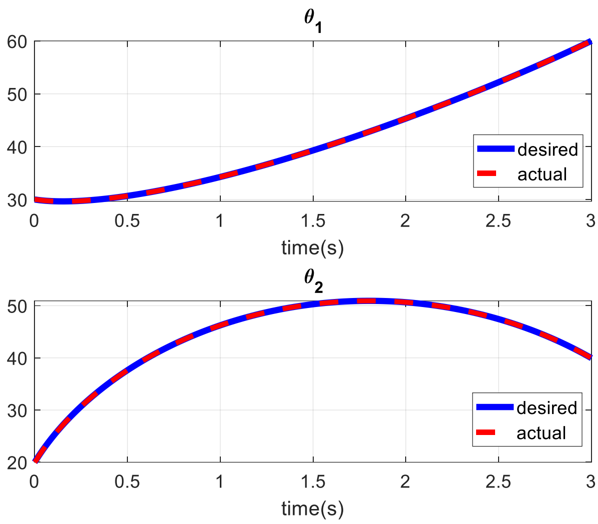

(a)

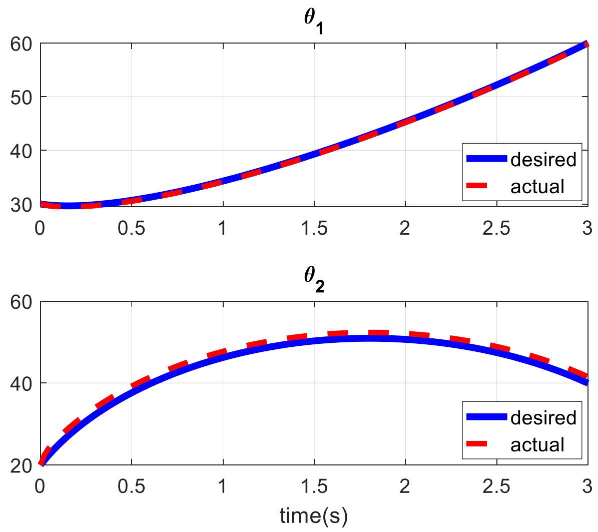

(b)

Figure 5. Comparison of the angular positions of the actual and desired conditions for each link (a) without external force, (b) with external force.

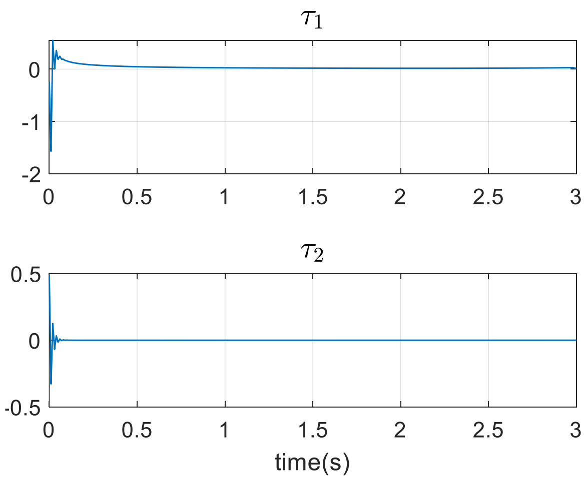

(a)

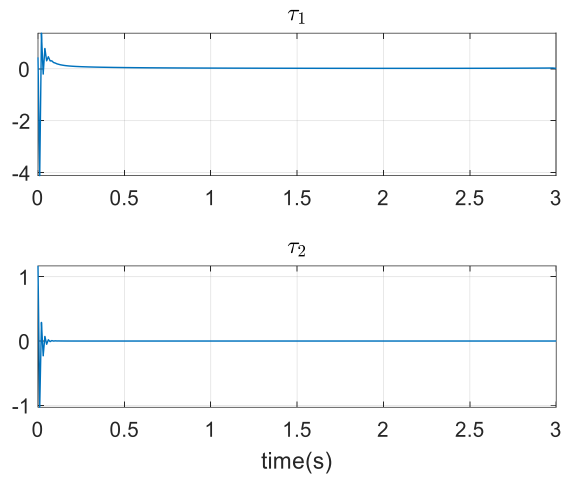

(b)

Figure 6. Comparison of the errors for each link (a) without external force, (b) with external force.

Results and Discussion

In this study, trajectory control of a SCARA robot with 2 DoFs was carried out under the influence of a certain external force acting on the tip of the robot through the trajectory line. For this, the MPC method, which is a very robust control method, was used. The PD control rule was preferred as the control law to be used in the MPC method. A trajectory line was created to be followed by the tip of the robot arm. An external force with constant magnitude was applied to the tip to be perpendicular to link 2 through the trajectory line. Performing some simulation studies, the desired and the controlled position graphs were obtained for both with and without external force conditions. The required input torques are larger for the case of external force as expected. According to the simulation results, the control of the robot for both cases was performed successfully by using the MPC method.

References

[1] R. H. Middleton and G. C. Goodw1n, “Adaptive computed torque control for rigid link manipulations,” *Syst. Control Lett.*, vol. 10, pp. 9–16, 1988.

[2] S. W. Wijesoma and R. J. Richards, “Robust Trajectory Following of Robots Using Computed Torque Structures with VSS”, *International Journal of Control*, 52 (1990), 4, pp. 935-962

[3] Z. Yang, J. Wu, J. Mei, J. Gao, and T. Huang, “Mechatronic Model Based Computed Torque Control of a Parallel Manipulator,” *Int. J. Adv. Robot. Syst.*, vol. 5, no. 1, pp. 123–128, 2008.

[4] O. O. Obadina, M. Thaha, K. Althoefer, and M. H. Shaheed, “A Modified Computed Torque Control Approach for a Master-Slave Robot Manipulator System,” *in Towards Autonomous Robotic Systems. TAROS 2018. Lecture Notes in Computer Science*, vol. vol 10965, M. Giuliani, T. Assaf, and M.

Giannaccini, Eds. Springer, Cham, 2018, pp. 28–39.

[5] M. Saad, P. Bigras, L. Dessaint, and K. Al-Haddad, “Adaptive Robot Control Using Neural Networks”, *IEEE Transaction on Industrial Electronics*, Vol.41, No: 2. 1994.

[6] M. Lee, and Y. Choi, “An Adaptive Neurocontroller Using RBFN for Robot Manipulators”, *IEEE Transaction on Industrial Electronics,* Vol.51, (2004).

[7] W. Sun and Y. Wang, “An Adaptive Fuzzy control for Robotic Manipulators”, *International Conference on Control, Automation, Robotics and Vision*, Kunming China, 1952-1956, (2004).

[8] S. H. Hsu and L. C. Fu, “Adaptive decentralized control of robot manipulators driven by current-fed induction motors”, *IEEE/ASME Trans. Mechatronic*, 10 (2005), 4, pp. 465-468.

[9] J. Cronin, J. M. Escano, S. Roshany-Yamchi and N. Canty, “Fuzzy-Based Generalized Predictive Control of a Robotic Arm”, *Proceedings, 25th IET Irish Signals & Systems Conference*, 2014.

[10] R. Wai, “Tracking Control Based on Neural Network Strategy for Robot Manipulator”, *Neurocomputing*, 51, 425-445, (2003).

[11] K. Lochan and B. K. Roy, “Control of Two-link 2-DOF Robot Manipulator Using Fuzzy Logic Techniques: A Review”, *Proceedings, 4 th International Conference on Soft Computing for Problem Solving,* Warsaw, Poland, 2014

[12] N. Mendes and P. Neto, “Indirect adaptive fuzzy control for industrial robots: a solution for contact applications”, *Expert Systems with Applications*, 42 (2015), 22, pp. 929-935

[13] W. He, Y. Chen and Z. Yin, “Adaptive neural network control of an uncertain robot with full-state constraints*”, IEEE Trans. Cybern*, 46 (2016), 3, pp. 620-629

[14] H. Chaudhary, V. Panwar, R. Prasad and N. Sukavanam, “Adaptive Neuro Fuzzy Based Hybrid Force/Position Control for an Industrial Robot Manipulator”, *Journal of Intelligent Manufacturing*, 27 (2016), 6, pp. 1299-1308

[15] M. Huseyinoglu and T. Abut, “Dynamic model and control of 2-dof robotic arm”, *European Journal of Technique (EJT)*, 8(2), 141-150. 2018.

[16] S. Choi, and J. Kim, “A Fuzzy-Sliding Mode Controller for Robust Tracking of Robotic Manipulators”, *Mechatronics,* Vol.7, 199-216, (1997).

[17] A. M. Mustafa, “Modeling, simulation and control of 2-R robot”, *Global Journals of Research in Engineering*, 14(H1), 49-54. 2014

[18] J. P. Perez, R. Soto, A. Flores, F. Rodriguez, and J. L. Meza, “Trajectory Tracking Error Using PID Control Law for Two-Link Robot Manipulator via Adaptive Neural Networks”, *Procedia Technology*, vol. 3, pp. 139–146, 2012. https://doi.org/10.1016/j.protcy.2012.03.015

[19] Q. Ma and X. Lei, “Dynamic Path Planning of Mobile Robots Based on ABC Algorithm”, *Lecture Notes in Computer Science*, pp. 267–274, 2010. https://doi.org/10.1007/978-3-642-16527-6_34

[20] P. V. Savsani and R. L. Jhala, “Optimal Motion Planning For a Robot Arm by Using Artificial Bee Colony (ABC) Algorithm”, *International Journal of Modern Engineering Research (IJMER),* vol. 2, no. 6, pp. 4434–4438, 2012.

[21] M. Aydin and O. Yakut, “Real-time control of triglide robot using sliding mode control method”, *Industrial Robot: An International Journal*, 45(1), 89-97, 2018.

[22] S. Aksungur, M. Aydin and O. Yakut, “Real-time PID control of a novel RCM mechanism designed and manufactured for use in laparoscopic surgery”, *Industrial Robot: An International Journal*, 47(2), 153-166, 2020.

[23] T. Abut and S. Soyguder, “Real-time control of bilateral teleoperation system with adaptive computed torque method”, *Industrial Robot: An International Journal*, 44(3), 299-311, 2017.

[24] T. Abut and S. Soyguder, “Optimal adaptive computed torque control for haptic-teleoperation system with uncertain dynamics”, *Proceedings of the Institution of Mechanical Engineers Part I: Journal of Systems and Control Engineering*, 236(4), 800-817, 2022.

[25] C. E. Garcia, D. M. Prett and M. Morari, “Model Predictive Control: Theory and Practice a Survey”, *Automatica*, Vol. 25, No. 3, pp. 335-3t8, 1989.

[26] M. Nauman, W. Shireen and A. Hussain, “Model-Free Predictive Control and Its Applications”, *Energies,* 15, 5131 2022 https://doi.org/10.3390/en15145131.

[27] S. Qina and T. A. Badgwell, “A survey of industrial model predictive control technology”, *Control Engineering Practice* 11 733–764, 2003

[28] L. A. Zadeh, and B. H. Whalen, “On optimal control and linear programming”, *IRE Trans. Aut. Control*, 7(4), 45, 1962.

[29] A. I. Propoi, “Use of LP methods for synthesizing sampled-data automatic systems”, *Automn Remote Control*, 24, 837, 1963.

[30] R. K. Mehra, R. Rouhani, J. Eterno, J. Richalet and A. Rault, “Model algorithmic control: review and recent development”. *Engng Foundation Conf. on*

Chemical Process Control II, Sea Island, Georgia, pp. 287-310, 1982.

[31] D. M. Prett and R. D.Gillette, "Optimization and constrained multivariable control of a catalytic cracking unit". *AIChE National Mtg*, Houston, Texas; also *Proc. Joint Aut. Control Conf.*, San Francisco, California, 1979.

[32] P. E. Orukpe, "Model Predictive Control Fundamentals", *Nigerian Journal of Technology*, Vol. 31, No. 2, pp. 139-148, 2012.

[33] Z. Houzhong, L. Jiasheng, Y. Chaochun, S. Xiaoqiang and C. Yingfeng, "Application of explicit model predictive control to a vehicle semi-active suspension system", *Journal of Low Frequency Noise, Vibration and Active Control*, 39(3) 772–786, 2020.

[34] S. S. Oyelere, "The Application of Model Predictive Control (MPC) to Fast Systems such as Autonomous Ground Vehicles (AGV)", *Journal of Computer Engineering*, 16(3), 27-37, 2014.

[35] G. B. Avanzini, A. M. Zanchettin and P. Rocco "Reactive Constrained Model Predictive Control for Redundant Mobile Manipulators", Advances *in Intelligent Systems and Computing book series* (AISC,volume 302).

[36] E. H. Guechi, S. Bouzoualegh, Y. Zennir and S. Bllazic, "MPC Control and LQ Optimal Control of A Two-Link Robot Arm: A Comparative Study", *Machines*, 6, 37, 2018.